Effect of drawing on the dielectric properties and polarization of pressed solution cast *β*-PVDF films

Aline Bruna da Silva · Celio Wisniewski · João Victor Almeida Esteves · Rinaldo Gregorio Jr.

Abstract Poly(vinylidene fluoride), PVDF, samples containing exclusively the polar β phase were obtained by crystallization from *N,N*-dimethylformamide (DMF) solution at 60 °C and subsequent pressing. Some of these samples were uniaxially drawn at 120 °C at draw ratio of 4, resulting in oriented films. Oriented and unoriented samples were characterized as to relative fraction of β phase, degree of crystallinity and orientation by infrared spectroscopy (FTIR), differential scanning calorimetry (DSC), and wide-angle X-ray diffraction (WAXD). The dependence on frequency of the real (ε_r') and imaginary (ε_r'') components of the relative permittivity of the samples was determined between 10^4 and 1.7×10^7 Hz. The coercive field and stable and metastable remanent ferroelectric polarization were determined from the hysteresis loop obtained by the ramp voltage technique, described in detail in this work. The results allowed verification of the effect of drawing on structure and of the resulting structure on the dielectric properties, remanent polarization, and coercive field of β-PVDF. A possible effect of the crystal–amorphous interphase region on the metastable remanent polarization is suggested. The results obtained with the oriented and unoriented samples were compared with those obtained for films commercialized by Piezotech S.A.

A. B. da Silva · J. V. A. Esteves · R. Gregorio Jr. (✉)
Department of Materials Engineering, Federal University of São Carlos, Rod. Washington Luís, Km 235, São Carlos, SP 13565-905, Brazil
e-mail: gregorio@ufscar.br

C. Wisniewski
Department of Physics, Federal University of Alfenas, Alfenas, MG 37130-000, Brazil

Introduction

Poly(vinylidene fluoride), PVDF, is a widely investigated semicrystalline polymer due to its attractive pyro and piezoelectric properties when polarized, in addition to its flexibility, excellent processibility, thermal stability, and chemical resistance. This polymer can crystallize into at least four distinct crystalline phases, known as α, β, γ, and δ. The crystalline structure and molecular conformation of these phases are well documented in the literature [1, 2]. Each crystalline phase confers characteristic properties to the polymer and therefore distinct applications. For technological applications like sensors and actuators the β-phase is preferred, because of its improved pyro and piezoelectric activity. However, the most readily obtained phase is α from melt crystallization. Films containing the β phase for applications like electroactive elements are commonly obtained by either uniaxial or biaxial drawing of originally α-phase films at draw ratios (R = ratio between final and initial length of the sample) between 3–5 and temperatures below 90 °C [3–7]. However, in this case the $\alpha \rightarrow \beta$ phase transformation is seldom complete and a fraction of α always remains. Crystallization from solution may yield exclusively the β phase, as long as evaporation rate is low, which depends on the temperature and solvent used [8–10]. However, the films obtained present increased porosity, which besides impairing mechanical and optical properties, make poling difficult. Sencadas et al. [11] showed that application of high pressure (15 MPa at 140 °C) normal to the surface of these films do not alter their crystalline phase and significantly reduces porosity, resulting in transparent films with good mechanical properties. In addition to allowing poling of the films, this procedure enables orientation through mechanical drawing. The dielectric, pyro, and piezoelectric properties of PVDF

are known to depend not only on crystalline phase, but also on crystallite orientation distribution. Uniaxial orientation of β-PVDF films obtained from solution and pressing orients the crystallite *c*-axis (direction of the polymer chains) preferentially in the draw direction [7]. This conformation favors orientation of the dipoles during poling when the electric field is applied perpendicularly to the film surface.

So far, no dielectric and ferroelectric characterization of exclusively β-phase films obtained from pressed solution cast PVDF films has been performed, either oriented or unoriented. The exclusive effect of drawing on remanent polarization of β-PVDF films has also not been observed yet, because β samples have always been obtained by mechanical drawing of originally α-phase films, and therefore always oriented. The purpose of the current work is to characterize the structure of exclusively β-phase films and to determine the dielectric (permittivity and loss index) and ferroelectric (remanent polarization and coercive field) properties, before and after drawing. In this way, it was possible to verify the effect of degree of crystallinity and of orientation on these properties. Utilization of the ramp voltage (RV) technique to determine the hysteresis loop enabled separation of the stable and metastable components of the total remanent ferroelectric polarization of PVDF, as well as verification of the effect of drawing on the relation between these polarizations. To verify reliability of the technique, films with known remanent polarization, commercialized by Piezotech S.A., were also characterized and the results compared with those obtained for the investigated samples.

Experimental

Materials and samples preparation

The PVDF resin used in this study, Foraflon® 4000HD, was supplied by Elf Atochem. This resin presented about 3.8 mol% of structural defects (head-to-head or tail-to-tail linkage), as analyzed by ^{19}F-NMR. PVDF films with thickness ranging from 20 to 40 μm were obtained from a 20 wt% *N,N*-dimethylformamide (DMF, Merck 99.5%) solution. The solution was kept at 60 °C under mechanical stirring up to complete dissolution of the PVDF. Next, it was cast and spread on a previously heated glass substrate, where it remained inside an oven for 2 h at 60 °C, resulting in evaporation of the solvent and crystallization of the polymer. The film was then removed from the substrate and submitted to uniaxial pressure of 150 MPa at 130 °C for 10 min, using a hydraulic press. Some of these films were submitted to uniaxial drawing at 120 °C, $R = 4$ and draw rate of 2×10^{-3} m/min, employing the device described in Ref. [7]. Sample thickness after drawing ranged from 15 to

Table 1 Preparation technique of each investigated sample

Sample	Preparation technique
A	Crystallized from solution at 60 °C and pressed at 130 °C and 150 MPa
B	Sample A drawn at 120 °C and draw ratio of 4
C	Film purchased from Piezotech S.A.

20 μm. For comparison's sake and to check reliability of the results, samples of uniaxially oriented films with thickness of 25 μm, commercialized by Piezotech S.A., were also used. Table 1 contains a summary of the preparation techniques of each investigated sample. For the electric measurements circular samples with a diameter of 7 mm were cut from the films obtained by the above-mentioned techniques. For the dielectric measurements aluminum electrodes were vacuum evaporated on both sides of the specimens. For the determination of the hysteresis loop specimens were used without electrodes.

Equipment

Transmission FTIR spectra were collected using a Perkin–Elmer Spectrum 1000 spectrophotometer, in the wave number range between 400 and 1000 cm^{-1} at a resolution of 2 cm^{-1}. FTIR measurements with polarized light were performed using a Perkin–Elmer wire grid polarizer. X-ray diffraction (WAXD) was carried out on a Rigaku Rotaflex diffractometer, with Cu Kα radiation and Ni filter, operated at 40 kV and 40 mA, with scanning range $10° \leq 2\theta \leq 50°$. The WAXD patterns were recorded by the equatorial scans with the incident X-ray beam directed parallel to the draw axis of the oriented film. Calorimetric analyses were conducted in a Perkin–Elmer DSC-7, calibrated with In, using samples of 6–8 mg and heating rate of 10 °C/min. Degree of crystallinity was evaluated by comparing the melt enthalpy of the sample obtained by DSC with that of 100% crystalline α-PVDF (104.5 J/g) [12]. The real (ε_r') and imaginary (ε_r'') components of the complex relative permittivity of PVDF were determined with a 4192A Impedance/Gain-Phase Analyzer, using a 16451B dielectric test fixture model, both from HP, in the frequency range between 10^4 and 1.7×10^7 Hz at ambient conditions ($T \approx 23$ °C and relative humidity $\approx 55\%$). Sample thickness was determined with a Dualscope MPOR from Fischer Instruments. The current profile and hysteresis loop were determined by the RV method, described next.

Detailed description of the RV method

The conventional method for determining the hysteresis loop uses the Sawyer and Tower [13] circuit where a
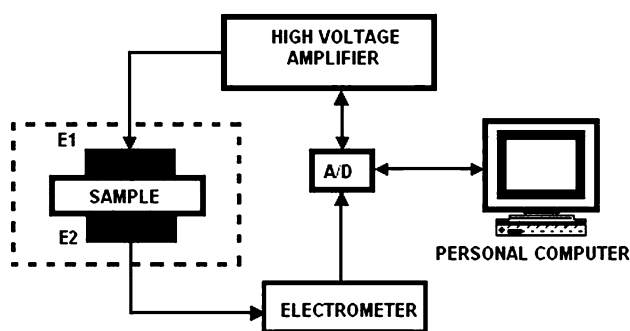
Fig. 1 Scheme of the hysteresis system used

bipolar, sinusoidal or triangle voltage is applied to the sample and the resulting current measured. In this work the RV method was used, developed by Wisniewski [14]. A scheme of the set-up used is illustrated in Fig. 1.

As voltage amplifier a 10/10B (10 kV) high-voltage amplifier from TREK was used, operating in amplifier mode. The sample was placed between two circular concentric brass electrodes with diameter of 7 mm (area = 3.85×10^{-5} m^2) and maintained in a closed system under vacuum (10^{-6} Torr) to prevent formation of an electric arc and consequent rupture of the sample during polarization. Between the sample and the brass electrodes a 0.5-mm thick conducting rubber (10^{-3} Ωm) with the same diameter of the electrodes was placed to improve coupling between the electrodes and the sample and minimize wrinkling of the sample during application of the voltage. No difference in the results was observed when using bare or aluminum-coated samples. Through the analog output of the A/D (National Instruments) board a time-variable voltage is generated and applied to the inlet of the high-voltage source. This source amplifies the signal 10^3 times and applies the amplified signal to the electrode E_1 of the sample. The resulting electric current is measured by the electrometer (Keithley 610C), which operates as a current/voltage converter and transforms the current signal into a voltage signal. A GPIB interface (Keithley Instruments) was used to control and acquire data from the electrometer. The reference voltage values and the output of the high-voltage source and of the electrometer are received by the A/D board and the data processed by the microcomputer. All measurements were performed at room temperature (≈ 23 °C). The samples were kept under vacuum for 4 h prior to polarization.

In the RV method, an adaption of the technique used by Dickens et al. [15], the sample is previously poled by applying successive bipolar (triangular) voltage cycles. At least twenty bipolar voltage cycles were applied until the current profile became repetitive. The sample was then negatively poled, i.e., the dipoles were oriented in the

direction opposite to the applied field during the measurements. After this procedure, a unipolar triangular voltage was applied to the sample (load), resulting in an average electric field in the sample (E) that varied linearly with time, and the resulting current was measured. Next, the sample remained short-circuited for a time t_c and a triangular voltage was again applied (reload) and the resulting current was measured. The two voltage cycles are represented in Fig. 2a. The value of $\frac{dE}{dt}$ was maintained constant during load and reload and depended on the maximum electric field applied to the sample. The load and reload times were always set at 200 s ($f = 5 \times 10^{-3}$ Hz).

Application of a time-variable electric field to a ferroelectric material, in which the effects of bound charges are negligible, yields as a response a current density given by:

$$J(t) = \frac{dD(t)}{dt} + J_c(t) \tag{1}$$

where $J_c(t)$ is the conduction current density and $D(t)$ the electric displacement, given by:

$$D(t) = \varepsilon E(t) + P(t) \tag{2}$$

Here ε is the dielectric permittivity of the sample and $P(t)$ the ferroelectric polarization, caused by dipole switching in the material. Substituting expression (2) in (1), the current density in the first cycle (load) where ferroelectric switching occurs will be given by:

$$J_1(t) = \varepsilon \frac{dE}{dt} + \frac{dP(t)}{dt} + J_c(t) \tag{3}$$

In the second cycle (reload), if short-circuit time is zero ($t_c = 0$) no ferroelectric switching occurs and the current density is given by:

$$J_2(t) = \varepsilon \frac{dE}{dt} + J_c(t) \tag{4}$$

Hence, considering equal times for load and reload (Fig. 2a) and that the capacitive component and conduction current are the same on load and reload, the ferroelectric polarization can be given by the following expression:

$$P(t) = \int_0^t [J_1(t) - J_2(t)]dt \tag{5}$$

If conduction current is negligible, on reload there will be only capacitive current J_{cap} (Fig. 2b), otherwise there will also be contribution of the conduction current $J_c(t)$ (Fig. 2c). Since the electric field is a function of time, the variation in polarization may be described as a function of the field $P(E)$. Hence, having determined the current densities $J_1(t)$ and $J_2(t)$, on load and reload, respectively, the variation in ferroelectric polarization as a function of the applied electric field can be determined by expression (5).

Fig. 2 Variation in voltage and current density with time in a typical RV measurement. The two cycles of unipolar triangular voltage on loading and reloading (**a**). The resulting current densities for a sample where the capacitive component predominates (**b**) and with the capacitive and conducting component of the same magnitude and a small polarization that relaxed during the short-circuit time (**c**)
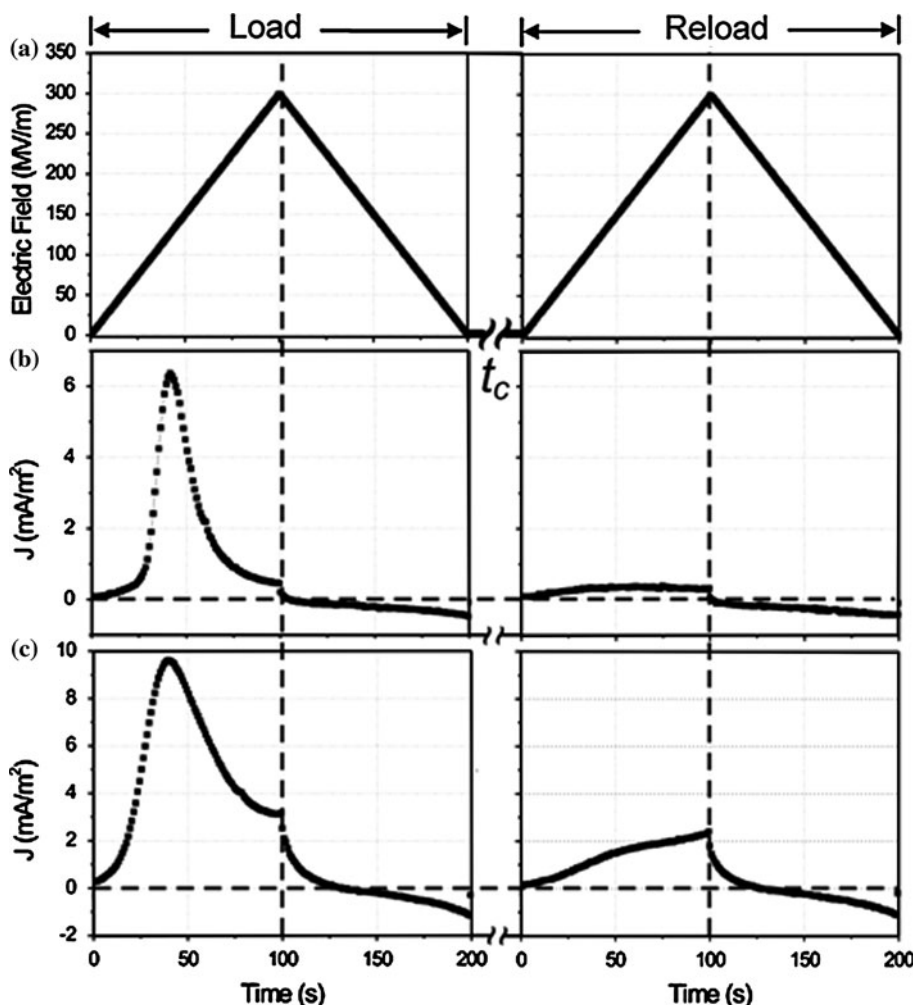
The component due to the capacitive current density is given by the expression:

$$J_{cap} = \varepsilon \frac{dE}{dt} \tag{6}$$

Since in the RV method the field varies linearly with time $\frac{dE}{dt}$ is a positive constant in the ascending ramp and negative in the descending ramp (Fig. 2a). Therefore, the capacitive current density is constant and allows calculation of ε or of the relative permittivity $\varepsilon'_r = \frac{\varepsilon}{\varepsilon_o}$, where ε_o is the permittivity of vacuum (=8.854×10^{-12} F/m), of the sample at frequency of 5×10^{-3} Hz.

Utilization of the constant current method to determine the hysteresis loop showed that the ferroelectric polarization of PVDF has a stable and metastable component [16, 17]. Wisniewski [14] showed that the metastable polarization relaxes within approximately 12 h after removal of the external electric field. In the conventional techniques used to determine the hysteresis loop the remanent polarization obtained includes the value of the metastable polarization. Utilization of the RV technique and a short-circuit time

above 12 h allows relaxation of the metastable polarization and reappearance during reload. In this way it is possible to separate the stable and metastable components of the total ferroelectric polarization. First, the total polarization (stable and metastable) of the sample is determined, integrating over time the difference between load and reload current density, with a zero short-circuit time between the two cycles. Next, the stable polarization is determined by the same procedure, however, with short-circuit time above 12 h between load and reload. The influence of the nonideal capacitive and conductive behavior of the sample is removed by subtraction of measured quantities. Effects of charge trapping in the sample that might occur during poling and that might be present in load and reload are also subtracted in the process.

Results

The samples were characterized as to the relative fraction of the β phase, chain orientation, and degree of crystallinity. To verify the relative fraction of the β phase in each
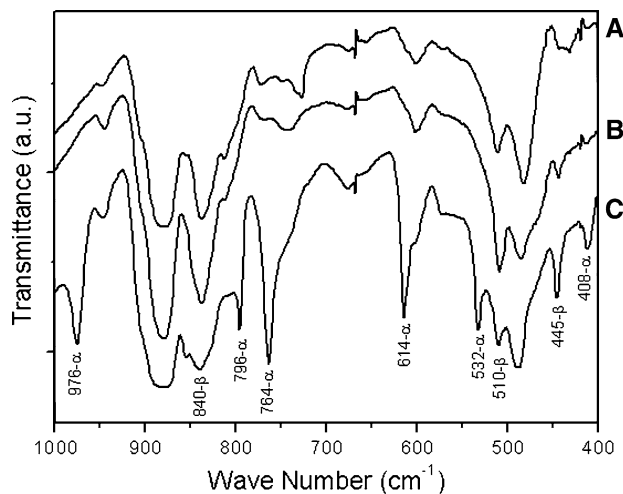
Fig. 3 FTIR spectra of samples *A*, *B*, and *C*. The characteristic bands of the α and β phases are presented in the figure

Fig. 4 FTIR spectra of samples *B* and *C* with radiation polarized parallel (∥) and perpendicular (⊥) to the draw direction

sample, FTIR spectra were obtained between the 400 and 1000 cm^{-1} region at room temperature. The results are presented in Fig. 3.

The solution cast film at 60 °C and pressed, before (A) and after drawing (B), presented characteristic absorption bands exclusively of the β phase (445, 510, and 840 cm^{-1}) [9, 18]. The film purchased from Piezotech (C) presented characteristic bands of both α (408, 532, 614, 764, 796, and 976 cm^{-1}) [9, 18] and β, demonstrating that this sample contains a mixture of both phases. The relative fractions of the β phase in each sample were estimated by the expression [8]:

$$F(\beta) = \frac{A_\beta}{1.26A_\alpha + A_\beta} \tag{7}$$

where A_α and A_β are the absorbance at 764 and 840 cm^{-1}, respectively. The results are shown in Table 2. Samples A and B present exclusively the β phase, whereas the fraction of β phase in sample C is only 0.45.

A comparison was made between chain orientation of films B and C by recording FTIR absorption in the wave number region between 2950 and 3050 cm^{-1} for radiation polarized parallel (∥) and perpendicular (⊥) to the draw direction (Fig. 4).

The 2980 and 3022 cm^{-1} bands correspond to the CH$_2$ symmetric and asymmetric vibration modes of PVDF,
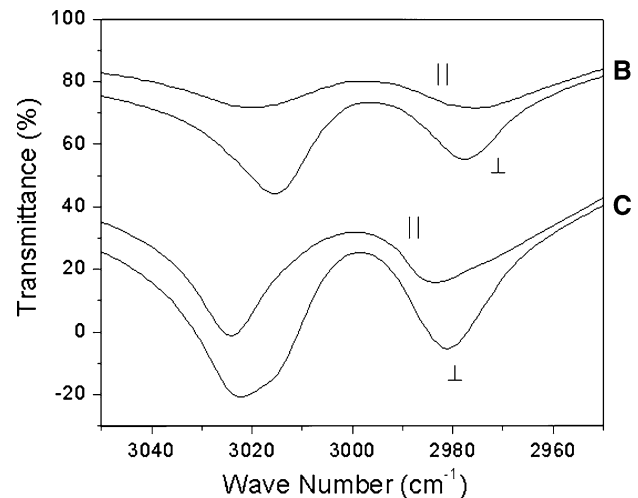
respectively [18]. The dipole associated with this group has a transition moment perpendicular to the PVDF chain direction. From the spectra one may determine the dichroism degree (D) [19] of these vibration modes, given by the ratio between absorbencies $A_\parallel$ and $A_\perp$, obtained for the electric field parallel and perpendicular to the draw direction, respectively. A lower value of D is expected for the sample with improved chain orientation in the draw direction. D values of samples B and C are listed in Table 2 referent to the two aforementioned bands. In relation to C, sample B is seen to present improved chain orientation in the draw direction. That is, in this sample the dipole moments have improved orientation in the direction perpendicular to drawing.

The degree of crystallinity of each sample was estimated by DSC. This assessment can only be made when negligible structural reorganization occurs during heating in the DSC run. Since in the uniaxial pressing process the samples were submitted to a temperature of 130 °C for 10 min, any possible structural reorganization that might have occurred during heating in the DSC run would already have occurred during pressing. Figure 5 shows DSC curves of the three samples and Table 2 contains the results obtained.

The melt temperatures (169 °C, endotherm peak) were similar for samples A and B, however, sample B presented a sharper endotherm. This result suggests that drawing

Table 2 Relative fraction of β phase [F(β)], dichroism degree (D), melt temperature (T$_m$), and degree of crystallinity (%C), by DSC and by X-ray diffraction, of the investigated samples

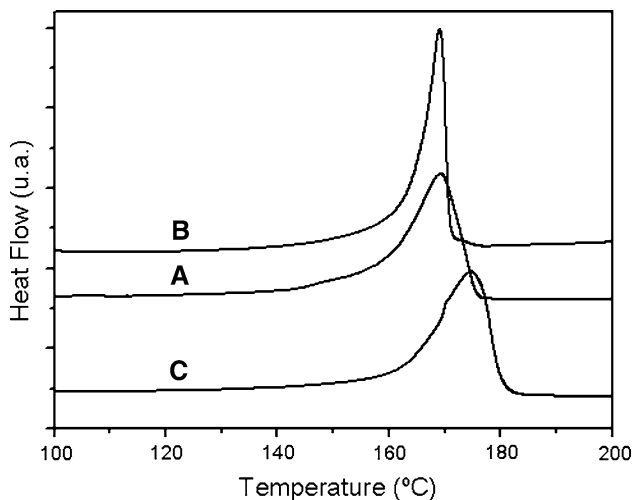| Sample	F (β)	D (2980 cm^{-1})	D (3022 cm^{-1})	T$_m$ (°C)	%C (DSC)	%C (X-ray)
A	1.0	–	–	169	59	47
B	1.0	0.37	0.28	169	60	63
C	0.45	0.50	0.55	175	63	–

Fig. 5 DSC curves of samples A, B, and C

induced reorganization of the metastable crystals, making them more stable and homogeneous. The enthalpies of fusion of these samples were very similar, resulting in practically equal degrees of crystallinity. Sample C presented a higher T_m (175 °C) and slightly higher degree of crystallinity. These differences were expected, since the Piezotech film was manufactured with a different PVDF resin and processed by another technique (blow molding).

Samples A and B were also submitted to X-ray diffraction (WAXD) and the diffractograms are shown in Fig. 6.

Both samples displayed a strong peak at $2\theta = 20.26°$ and a weaker one at 36.29°, characteristic of the β phase of PVDF [3, 20], corroborating FTIR results. The degree of crystallinity of samples A and B was also evaluated by
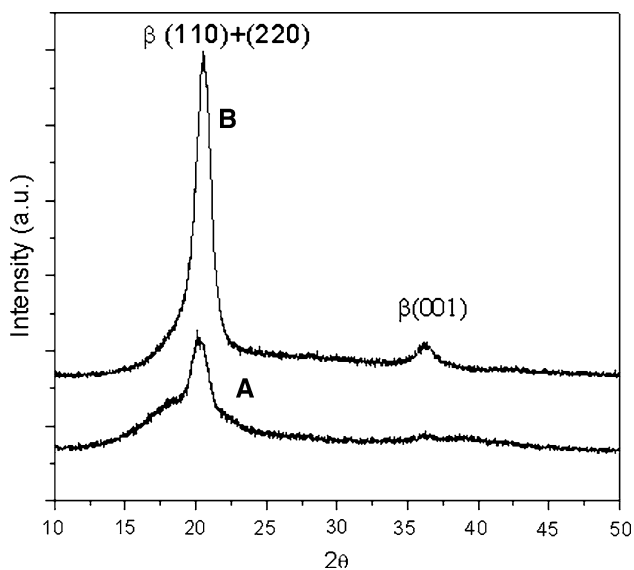
X-ray diffraction through the ratio of the sum of the peak areas and the total area of the diffractogram; results are shown in Table 2. The apparent disagreement between DSC and X-ray results of sample A are discussed in the next section.

Variation in ε'_r and in ε''_r in the frequency range between 10^4 and 1.7×10^7 Hz is shown in Fig. 7a and b, respectively. The values of ε'_r and ε''_r at 10 kHz and of the relaxation frequency (f_r, ε''_r peak) are shown in Table 3.

Variation in current density with electric field intensity on loading and reloading was determined by the RV method. Figures 8, 9, and 10 show (a) variations in current density at $t_c = 24$ h and (b) hysteresis loops at $t_c = 0$ and $t_c = 24$ h, for samples A, B, and C, respectively. The rectangular shape of the hysteresis loop is a consequence of the technique used, which subtracts from the result all polarizations that relax when the electric field is removed. The value of the coercive field was considered that which divides in half the peak area of the polarization current
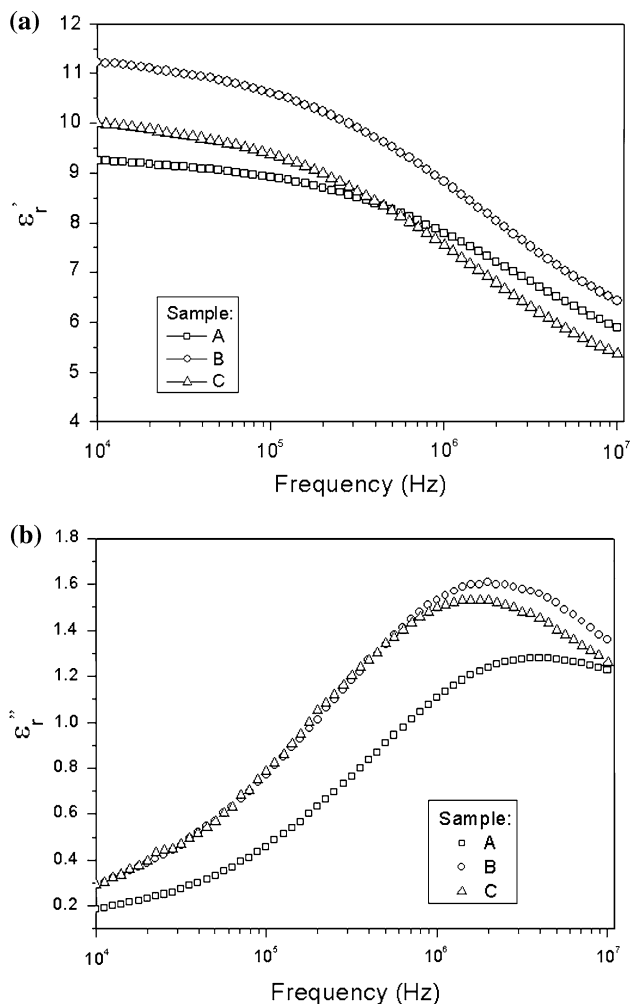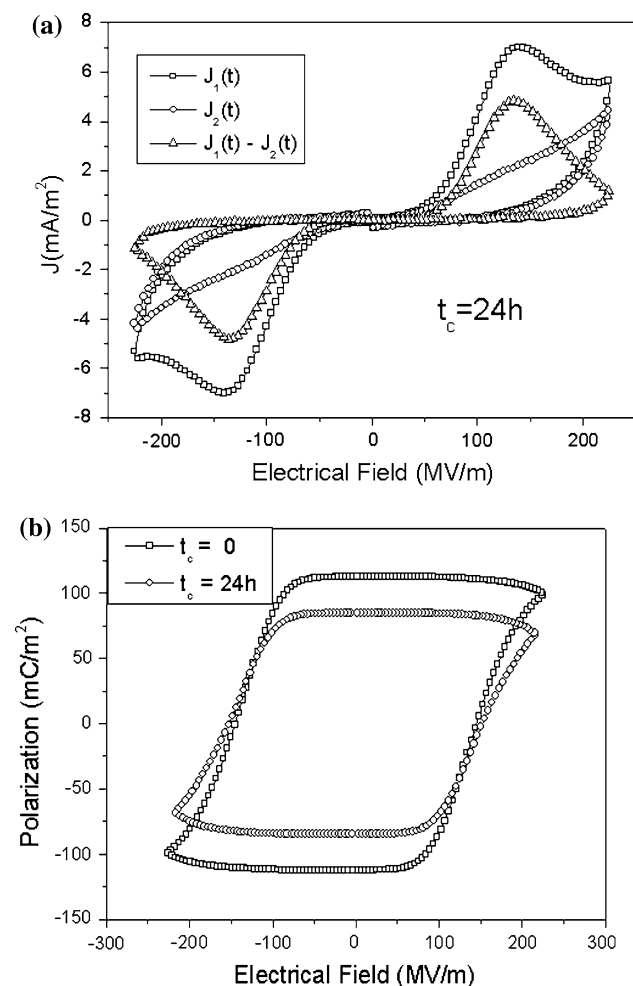

Fig. 6 WAXD spectra of samples A and B

Fig. 7 Variation in ε'_r (a) and ε''_r (b) as a function of frequency for samples A, B, and C

Table 3 Relative permittivity at 10 kHz and at 5×10^{-3} Hz, relaxation frequency (f_r), coercive field (H_c), and stable (P_r) and metastable (P_r') remanent ferroelectric polarization of the investigated samples

Sample	ε_r' (10 kHz)	ε_r' (5×10^{-3} Hz)	f_r (MHz)	H_c (MV/m)	P_r (mC/m²)	P_r' (mC/m²)
A	9.3	16	3.98	139	85	27
B	11.2	36	2.10	135	138	33
C	10.0	18	1.68	124	70	8

Fig. 8 **a** Current density profiles of load (*square*), reload (*circle*), and the difference between these (*triangle*) and **b** hysteresis loops at $t_c = 0$ (*square*) and 24 h (*diamond*), for sample A

Fig. 9 **a** Current density profiles of load (*square*), reload (*circle*), and the difference between these (*triangle*) and **b** hysteresis loops at $t_c = 0$ (*square*) and 24 h (*diamond*), for sample B

density, i.e., the field that inverts the direction of half of the previously oriented dipoles. Values of coercive field and of stable and metastable remanent polarization (difference between remanent polarization at $t_c = 0$ and $t_c = 24$ h) of the three samples are listed in Table 3.

The current load density $J_1(t)$ increases, reaches a maximum and decreases to the sum of the conduction and capacitive currents, evidencing the occurrence of switching. This behavior coincides with that theoretically predicted by Buchman [21] for this process. From the current
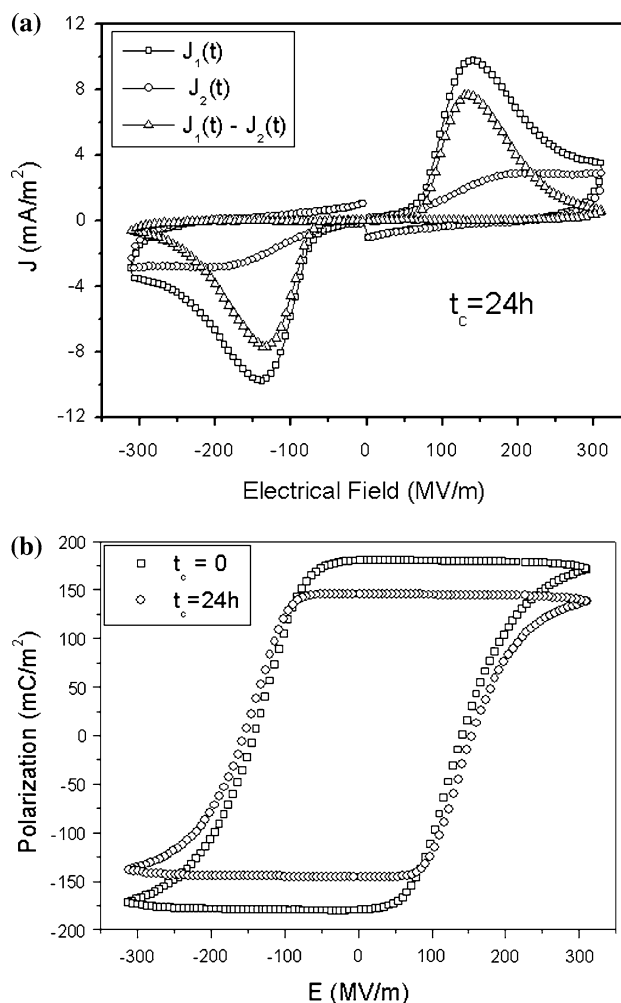
reload density $J_2(t)$ profiles it can be seen that after short-circuit time of 24 h samples A and B presented metastable polarization, in addition to the capacitive and conduction components. For sample C the metastable polarization and the conduction current were neglected, remaining practically only the capacitive component. The high ionic conductivity of samples A and B is likely related to adsorbed water and residual solvent in these samples which may originate charge carriers. The total remanent polarization
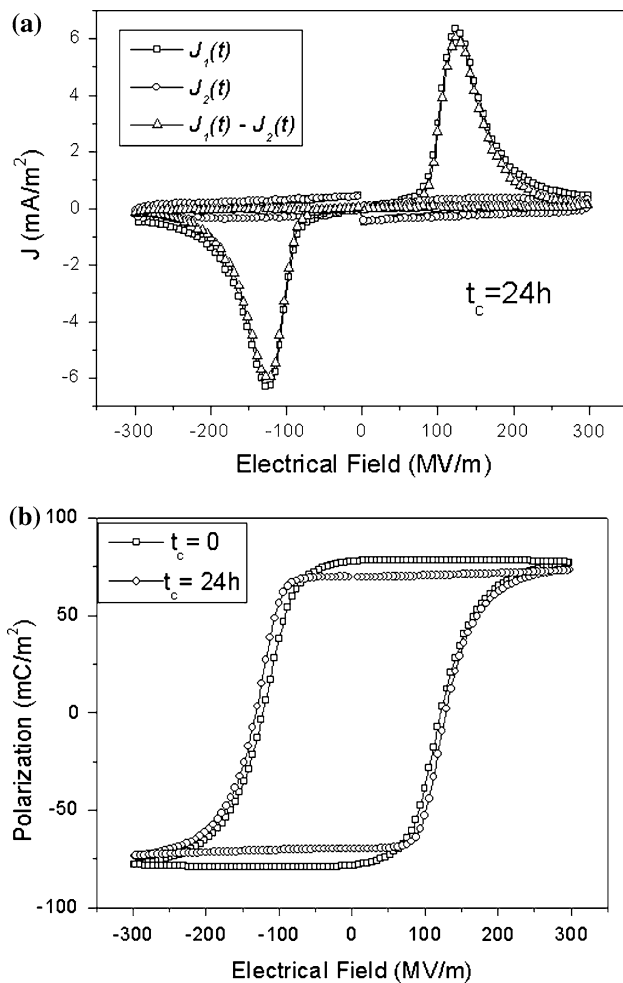
Fig. 10 **a** Current density profiles of load (*square*), reload (*circle*), and the difference between these (*triangle*) and **b** hysteresis loops at $t_c = 0$ (*square*) and 24 h (*diamond*), for sample C

$(P_r + P'_r = 78 \, \text{mC/m}^2)$ obtained for sample C is very close to that encountered in the literature for Piezotech films [22], corroborating reliability of the results obtained by the RV technique. The high conductivity of sample A impeded application of an electric field above 220 MV/m without rupturing the sample and, therefore, the maximum polarization of this sample could not be obtained. Even so, the stable ferroelectric polarization of this sample was superior to that obtained for sample C. To sample B it was possible to apply an electric field of up to 307 MV/m, likely due to the lower electric conductivity of this sample. In the drawing process this sample remained at 120 °C for 15 min and this annealing process likely favored removal of the adsorbed water and residual solvent, permitting maximum polarization of the sample. Comparison of the results for samples A and B shows that drawing increased the stable ferroelectric polarization and reduced the percentage of the metastable component in relation to the total polarization.

The value of the capacitive current, obtained at $E = 0$ at the end of reload, and expression (6) were used to determine ε'_r of samples A, B, and C at $f = 5 \times 10^{-3}$ Hz. Values are listed in Table 3. The higher value of ε'_r at 5×10^{-3} Hz compared to that at 10 kHz was already expected, since at lower frequencies there is the contribution of other polarizations, such as interfacial polarization (Maxwell–Wagner–Sillars (MWS) polarization). For α-PVDF films and 10^{-1} Hz, Tuncer et al. [23] obtained $\varepsilon'_r = 21$. Singh et al. [24] obtained $\varepsilon'_r = 16$ at 10^2 Hz for a PVDF sample cast from solution at 80 °C and uniaxially drawn at 150 °C, containing a mixture of α and β phase. These values are very close to those obtained for samples A and C. The value of $\varepsilon'_r = 36$ obtained for sample B indicates the occurrence of a stronger polarization, likely interfacial. The reason for this high polarization in this sample is still under investigation. One of the advantages of the RV technique is the simultaneous determination of the stable and metastable ferroelectric polarization and of the permittivity of the material at the applied alternated field frequency.

Discussions

The evaluation of crystallinity of sample A by DSC and by X-ray diffraction showed an apparent disagreement between the results obtained. However, it should be pointed out that the endotherm area in DSC analysis included not only the energy required to melt the crystalline region of the polymer but also the crystal–amorphous interphase. The existence of this interphase was first evidenced by Flory [25]. At this interphase, intermediate between the crystalline and amorphous region, the chains are less organized and not so strongly bound as the crystalline phase. Hence, the temperature required to destroy chain order in this region is lower than in the crystalline phase and the fusion enthalpy of this region corresponds to the area at the onset of the endotherm. So, the total endotherm area of sample includes this enthalpy and yields a higher crystallinity than the actual one. In X-ray analysis the peaks referent to the diffractions depend on the interplanar distances, characteristic of the crystal and are therefore only related to the crystalline region. Therefore, for undrawn sample A the degree of crystallinity closest to the actual one is likely that obtained by X-ray diffraction (47%), because that obtained by DSC (59%) includes the interphase region. In the drawn sample B the degree of crystallinity obtained by WAXD (63%) might have included the pseudo-ordered region caused by drawing, yielding a higher value than the actual one. On the other hand, the endotherm obtained for this sample was narrower and presented a higher onset melt temperature, evidencing the

existence of more homogeneous and more stable crystals. This result indicates that drawing, on orienting the chains in the interphase region, may have caused reorganization of the crystals and part of the chains that belonged to the interphase became more ordered and hence became part of the crystalline region. Annealing experienced by the sample during drawing (15 min at 120 °C) may have contributed to this transformation. Therefore, for sample B the crystallinity obtained by DSC (60%) seems to be closer to the actual value than for sample A. With these considerations it can be concluded that drawing sample A increased its degree of crystallinity from 47% to a value between 60 and 63%, due to the fact that part of the interphase region became crystalline.

It was verified that ε_r' and ε_r'' increased with chain orientation caused by drawing. These results agree with those obtained in a previous work [3]. Drawing destroys the characteristic spherulitic structures of PVDF, forming a fibril morphology [4] with the chains preferentially aligned in the draw direction, parallel to the film surface [7]. The increase in ε_r' likely occurs because this alignment causes improved chain order of the amorphous phase, favoring packing of the molecule, reducing free volume, and increasing dipole density. Alignment of the chains also favors orientation of the dipole moments, normal to the chains, when the external electric field is applied perpendicularly to the sample surface. Both effects contribute to the increase in ε_r' and ε_r''. However, the reduction in free volume caused by drawing reduces chain mobility and shifts the relaxation frequency to lower values.

Analysis of the hysteresis loops of samples A and B show that drawing increased the stable ferroelectric polarization and reduced the metastable one. Since both samples present exclusively the β phase the increase in stable polarization likely occurred in part due to the increase in crystallinity of sample B, since previous experiments [26–30] indicate that this polarization originates mainly from dipole orientation in the crystalline region of PVDF, even though injected charges may affect the process [31]. In addition, the preferential orientation of the chains in the draw direction, and consequently of the dipoles in the perpendicular direction, also favors polarization. The percentual decrease in metastable ferroelectric polarization is likely related to the reduction in the interphase region caused by drawing, evidenced by the different endotherms of samples A and B. It is, therefore, likely that the metastable polarization occurs in this region where the chains are not as strongly bonded as in the crystalline region, allowing relaxation of the dipoles some hours after removal of the external electric field.

Sample C, purchased from Piezotech presented the lowest remanent stable ferroelectric polarization. This occurred because this sample, despite presenting the highest degree of crystallinity (63%), possesses the lowest relative fraction of phase β (0.45), even though the α phase, converted to its polar version, has likely also contributed. This sample, on the other hand presented the lowest percentage of metastable polarization, probably because it has a smaller interphase region, which might be related to its processing.

These results confirm that in PVDF the main responsible factor for the strong stable remanent polarization is dipole orientation in the crystalline region. In this region chain bonding is so strong that the conformational changes required to alter the direction of the associated electric dipole moments hardly occur at room temperature. Therefore, the coercive field of the ferroelectric polymers is much higher (50–160 MV/m, depending on the temperature) than that of ceramics (1–3 MV/m). In the latter, polarization occurs due to atomic shifts inside the crystal; a process that requires much less energy (and time) than that necessary for conformational changes of the chains in the crystalline region of polymers. Hence, at room temperature, when the dipoles in the crystalline region of PVDF are oriented by the electric field, polarization remains stable for a long time after removal of the field. Since the dipole moment perpendicular to chain direction of the β crystalline phase (7.0×10^{-30} Cm) is higher than that of the α phase (4.0×10^{-30} Cm), the former has a higher remanent polarization. However, even the α phase may present ferroelectricity when it is poled by a field with an intensity (>1.25 MV/m) that allows transition to its polar version δ [32].

In the crystal–amorphous interphase region the dipoles are not as strongly bonded as in the crystalline region and after removal of the external electric field they are able to relax in few hours, reducing the total ferroelectric polarization. Therefore, the main responsible factor for the metastable ferroelectric polarization observed in PVDF is likely dipole orientation in this region and not the polarization caused by accumulated charges at the crystal–amorphous interface (MWS), as suggested by some authors [33].

The maximum theoretical polarization for 100% crystalline PVDF-β may reach up to 220 mC/m^2, if polarizability of the dipoles is taken into account [34]. So, sample A with 47% crystallinity would have a maximum theoretical polarization of 103 mC/m^2, higher than the value obtained (85 mC/m^2). This result is likely related to the low intensity of the maximum applied field, which did not allow complete polarization of the sample. Moreover, the chains in this sample are not oriented, which also disfavors polarization. Sample B, with crystallinity between 60 and 63%, would have maximum theoretical polarization between 132 and 139 mC/m^2. The value obtained (138 mC/m^2) shows that the crystallinity of this sample is

likely very close to 63% obtained by X-ray diffraction and that practically all dipoles were oriented. This value is much higher than those normally obtained for samples originated from drawn PVDF-α films (50–85 mC/m^2) [22, 29]. Even highly oriented PVDF-β films obtained by special techniques (cold drawing followed by annealing [35] or solid-state coextrusion [36]) presented remanent polarization between 85 and 100 mC/m^2, lower than that presented by sample B. It should be noted that these values refer to the total polarization, including the metastable component. The high value of P_r presented by sample B is likely due to the higher degree of crystallinity and improved chain orientation in this sample, in addition to the fact that it presents exclusively the β phase. The strong maximum electric field used in this work ($\cong 300$ MV/m) likely also has a contribution, as it caused improved dipole orientation. Considering the fact that the pyro and piezo-electric activities of PVDF are proportional to the remanent polarization, it is very likely that these activities are stronger in pressed and drawn solution cast films than in films obtained either by drawing originally α-phase film or by the aforementioned special techniques.

Conclusions

Pressed solution cast PVDF films containing exclusively the polar β phase presented stable remanent polarization superior to that obtained by β-phase samples originating from drawing α-PVDF films. Drawing the former films showed to increase permittivity and stable remanent polarization and to reduce the metastable component. Increase in permittivity was attributed to the increase in dipole density and improved chain orientation in the amorphous regions of the polymer. Increase in the stable polarization was attributed to the increase in crystallinity and improved orientation of the crystallites. The percentage of metastable polarization decreased with drawing, likely due to the reduction of the crystal–amorphous interphase region which might be accounted for this polarization. The drawn pressed solution cast films presented stronger stable remanent polarization when compared to films obtained by other techniques and, consequently, should present better pyro and piezoelectric activity.

References

1. Nalwa HS (1995) Ferroelectric polymers: chemistry, physics and applications. Marcel Dekker, New York
2. Lovinger AJ (1982) In: Basset DC (ed) Developments in crystalline polymers. Applied Science Publishers Ltd, London
3. Gregorio R Jr, Ueno EM (1999) J Mater Sci 34:4489. doi: 10.1023/A:1004689205706
4. Sencadas V, Moreira VM, Lanceros-Mendez S, Pouzada AS, Gregorio R Jr (2006) Adv Mater Forum III (514–516):872
5. Sajkiewicz P, Wasiak A, Goclowski Z (1999) Eur Polym J 35:423
6. Grubb DT, Kearney FR (1990) J Polym Sci B 28:2071
7. Branciforti MC, Sencadas V, Lanceros-Mendez S, Gregorio R Jr (2007) J Polym Sci B 45:2793
8. Gregorio R Jr, Cestari M (1994) J Polym Sci B 32(5):859
9. Gregorio R Jr (2006) J Appl Polym Sci 100(4):3272
10. Gregorio R Jr, Borges DS (2008) Polymer 49:4009
11. Sencadas V, Gregorio R Jr, Lanceros-Mendez S (2006) J Non-Crystal Solid 352:2226
12. Nakagawa K, Ishida Y (1973) J Polym Sci 11:2153
13. Sawyer CB, Tower CH (1930) Phys Rev 35:269
14. Wisniewski C (1999) Caracterização de Polímeros Ferroelétricos: Metodologia e Resultados. PhD Thesis, University of São Paulo, São Carlos, SP
15. Dickens B, Balizer E, DeReggi AS, Roth SC (1992) J Appl Phys 72(9):4258
16. Giacometti JA, Wisniewski C, Ribeiro PA, Moura WA (2001) Rev Sci Instrum 72(11):4223
17. Wisniewski C, Ferreira GFL, Moura WA, Giacometti JA (2000) J Phys D 33:2483
18. Kobayashi M, Tashiro K, Tadokoro H (1975) Macromolecules 8(2):158
19. Bower DI (2002) An introduction to polymer physics. Cambridge University Press, Cambridge
20. Das-Gupta DK, Doughty K (1978) J Appl Phys 49(8):4601
21. Buchman P (1973) Ferroelectrics 5(1–2):39
22. Ueberschlag P (2001) Sens Rev 21(2):118
23. Tuncer E, Wegener M, Gerhard-Multhaupt R (2005) J Non-Cryst Solid 351:2917
24. Singh R, Kumar J, Singh RK, Kaur A, Sinha RP, Gupta NP (2006) Polymer 47(16):5919
25. Flory PJ (1949) J Chem Phys 17:223
26. Naegele D, Yoon DY (1978) Appl Phys Lett 33(2):132
27. Tamura M, Hagiwara S, Matsumoto S, Ono N (1977) J Appl Phys 48(2):513
28. Scheinbeim JI, Chung KT, Pae KD, Newman BA (1979) J Appl Phys 50(10):6101
29. Furukawa T, Date M, Fukada E (1980) J Appl Phys 51(2):1135
30. Takahashi T, Date M, Fukada E (1980) Appl Phys Lett 37(9):791
31. Sussner H, Dransfeld K (1978) J Polym Sci 16:529
32. Davis GT, McKinney JE, Broadhurst MG, Roth SC (1978) J Appl Phys 49(10):4998
33. Rollik D, Bauer S, Gerhard-Multhaupt R (1999) J Appl Phys 85(6):3282
34. Broadhurst MG, Davis GT (1980) In: Sessler GM (ed) Electrets. Springer-Verlag, Berlin, Heidelberg, New York
35. Takase Y, Scheinbeim JI, Newman BA (1989) J Polym Sci B 27(11):2347
36. Nakamura K, Nagai M, Kanamoto T, Takahashi Y, Furukawa T (2001) J Polym Sci B 39(12):1371